Anatomy and Physiology of the Nasal Valves

Derek H. Liu, MD[a], Hailey Chen[a], Brian J-F. Wong, MD, PhD[a,b,c,d,*]

KEYWORDS

• Internal nasal valve • External nasal valve • Lateral wall insufficiency
• Dynamic valve collapse • Nasal obstruction

KEY POINTS

- The external nasal valve is defined by the cross-section of the ala, whereas the internal nasal valve is defined by the septum, caudal margin of the upper lateral cartilage, and the inferior turbinate.
- Nasal valve function is defined by complex, 3-dimensional structures composed of cartilage, muscle, connective tissue, and skin which provide both static and dynamic support.
- Normal nasal airflow has been described with widely accepted concepts, including a critical internal nasal valve angle, the Bernoulli principle, and Poiseuille's equation, which may be insufficient to capture the 3-dimensional, patient-specific nature of nasal obstruction.
- Computational fluid dynamics has emerged as a potential noninvasive technique for assessing nasal valve physiology while accounting for the complexities of the nasal airway geometry.

THE NASAL VALVE

Mink first described the nasal valve in 1903 as a region of narrowing in the nasal vestibule. He defined the nasal valve as a region bounded medially by the septum and laterally by the limen nasi, where the caudal border of the upper lateral cartilage (ULC) overlaps the lateral crus of the lower lateral cartilage (LLC).[1–3] Since then, there has been variation in the use of the term "nasal valve." Most commonly, authors refer to 2 separate regions within the nasal vault as the external nasal valve (ENV) and internal nasal valve (INV) (**Fig. 1**).

The ENV is operationally defined simply as the 2-dimensional (2D) cross-section of the ala. The borders are composed of the lateral crura of the LLCs, the columella and medial crura medially, and the nasal floor inferiorly.[1] Some have defined the external

[a] Department of Otolaryngology, Head and Neck Surgery, University of California Irvine, 101 The City Drive South, ZOT 5386, Orange, CA 92868, USA; [b] Beckman Laser Institute, University of California Irvine, Irvine, CA, USA; [c] Department of Biomedical Engineering, Samueli School of Engineering, University of California Irvine, Irvine, CA, USA; [d] Facial Plastic Surgery
* Corresponding author. 101 The City Drive South, ZOT 5386, Orange, CA 92868.
E-mail address: bjwong@uci.edu

Otolaryngol Clin N Am 58 (2025) 189–203
https://doi.org/10.1016/j.otc.2024.09.001 oto.theclinics.com

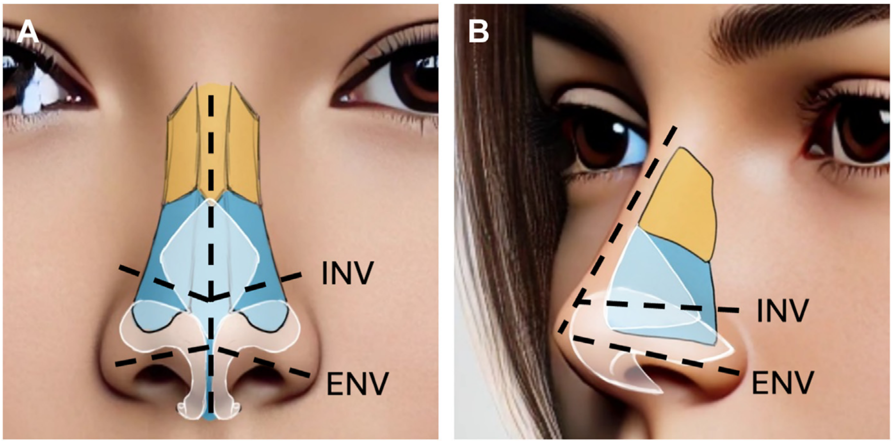

Fig. 1. External and internal nasal valves, (*A*) frontal and (*B*) oblique views. The ENV is located at the ala, while the INV is at the level of the caudal border of the ULC. ENV, external nasal valve; INV, internal nasal valve.

valve as a 3-dimensional (3D) volume, bordered caudally by the nostril anteroinferiorly and the internal nasal valve posteriorly.[4,5]

Most definitions of the INV demarcate this region as the plane through the nasal vault with the smallest cross-sectional area (CSA). Historically, the INV is defined by the septum medially, the caudal margin of the ULC laterally, and the inferior turbinate inferiorly. Typically located 1.3 cm deep into the nasal cavity, the INV angle delineated by the ULC and septum typically measures 10° to 15° in the Caucasian population. In practice, precise identification of the valve is difficult both clinically and even using diagnostic imaging (eg, CT). Valve angle measurement using the naked eye is, at best, a crude estimate.

ANATOMY

Muscles

The muscles of the nose can be organized as intrinsic, with origins and insertions contained within the nasal region, or extrinsic, which are outside this domain but act to alter nasal shape position (**Fig. 2**).[6] They can be classified by function, as listed below.[7] Some have also included the zygomaticus minor and orbicularis oris as relevant to nasal dynamics.[8]

1. Elevators: procerus, levator labii superioris alaequae nasi, and anomalous nasi
2. Depressors: alar nasalis (dilator naris posterior) and depressor septi nasi
3. Compressors: transverse nasalis and compressor narium minor
4. Dilators: dilator naris anterior

Electromyographic studies highlighted the role of specific nasal muscles in nasal valve function.[9,10] The nasalis forms the muscular component of the nasal superficial musculoaponeurotic system (SMAS).[11] The transverse portion, known as the pars transversalis, attaches to the nasal skin and indirectly stabilizes the nasal valve and sidewall. The alar portion, known as the par alaris and alternatively referred to as the dilator naris posterior, originates from the maxilla and attaches to the accessory cartilage medially, providing lateral stability of the ala.[12,13] The dilator naris anterior,

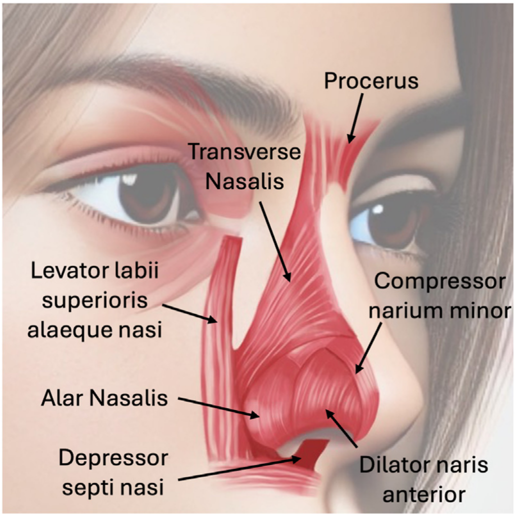

Fig. 2. Muscles of the nose.

also referred to the apices nasi, originates from the lateral crus to attach to the alar groove. Previous studies disagreed regarding the presence of an independent dilator naris muscle, with some recent studies referring to a dilator naris vestibularis which occupies and surrounds nearly the entire nasal ala.[14–18]

The importance of nasal muscles function is best illustrated in patients with facial nerve injury, who often experience nasal obstruction. While a significant contributor to nasal valve collapse is the weight of the unsupported cheek tissues, the nasal muscles both actively flare the nostrils and provide static support against gravity.[13,19] For example, temporary paralysis of nasal muscles with lidocaine results in reductions in alar stiffness along with flow restriction measured by rhinomanometry. This suggests that resting muscle tone is critical in supporting nasal airway patency.[20] Loss of muscular activity results in ENV narrowing and collapse, and surgical interventions for facial paralysis patients such as suture suspension or fascia lata slings are associated with improved Nasal Obstruction and Septoplasty Effectiveness (NOSE) survery scores.[21]

Lower Lateral Cartilages

The paired LLCs are divided into 3 segments: the medial, intermediate, and lateral crura. The LLCs define the structure and shape of both the nasal tip and the ENV. The shape of the LLC is complex and defies taxonomy. Functionally, the LLC is a dome-shaped structure that maintains the nasal aperture and functions to resist forces of deformation generated during inspiration. One specific LLC morphology, alar malposition, warrants further discussion. Malpositioned lateral crura, now referred to more specifically as cephalic malposition, were a concept first defined by Sheen and Sheen.[22] The axis of the lateral crus may be defined as a line which begins at the dome medially and roughly bisects the length of the lateral crura (**Fig. 3**A–D). This axis should be oriented toward the lateral canthus of the ipsilateral eye. Cephalically malpositioned lateral crura have an axis which points toward the ipsilateral medial canthus.[23] In other words, cephalic lateral crura are more perpendicular to the alar rim, rather than parallel.

Cephalic malposition is associated with tip bulbosity and the compound tip deformity, external valve weakness, and collapse.[24] Constantian estimated that 50% of

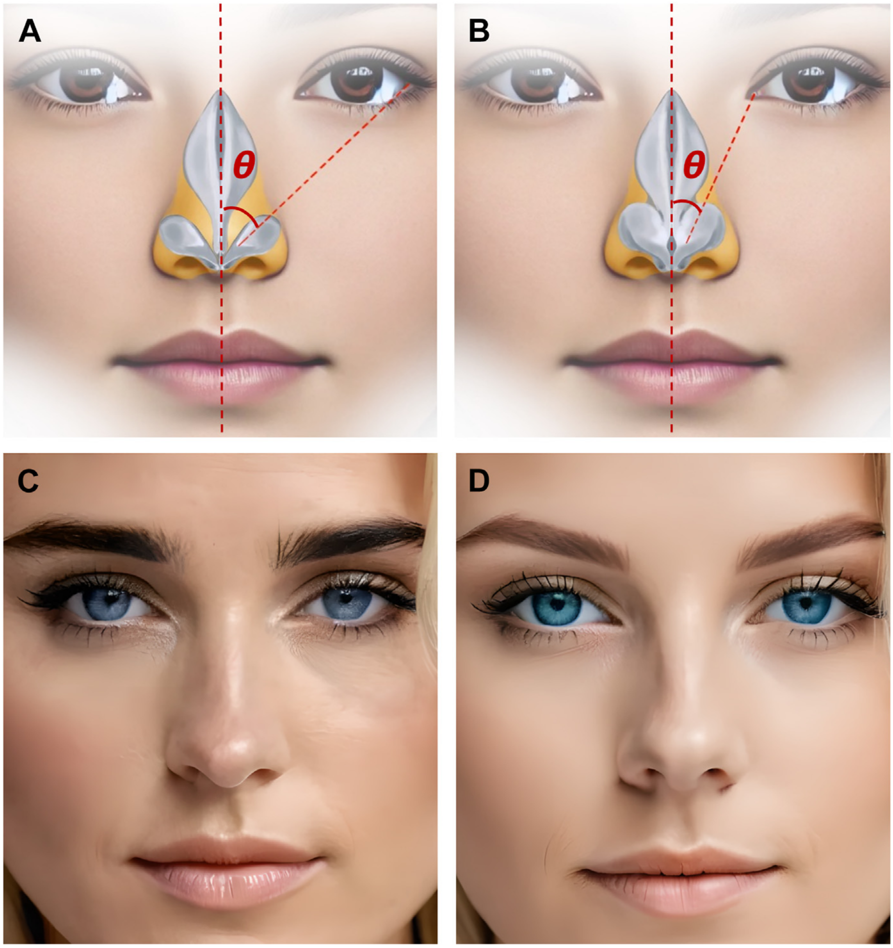

Fig. 3. Orientations of the lower lateral crus longitudinal axis (*A*) toward the lateral canthus (*B*) cephalically malpositioned toward the medial canthus (*C*) nasal tip with appropriately positioned lower lateral crura (*D*) malposition resulting in a broad nasal tip.

patients with external valve obstruction had cephalic lateral crura.[25–27] Different treatment strategies have been proposed, including repositioning of the lateral crura.[28] Using this technique, Toriumi advocated that the axis of the lateral crus and the mid-sagittal plane should ideally form an angle greater than 30°.[24,29] Lateral crural tensioning (LCT) can also accomplish this objective of improving the airway. First described by Davis, this technique combines a lateral crural steal with a caudal septal extension graft to increase tension and stabilize the sidewall.[30] Combining this tensioning with articulated alar rim grafts to support the alar margin, LCT may achieve similar improvements in airway but requires less cartilage and is potentially less likely to crowd the airway when compared with lateral crural strut grafts (LCSG).[31–35]

Upper Lateral Cartilages

The ULCs are paired, triangular cartilages which articulate with the septum medially, the pyriform aperture cephalically, and the LLCs caudally.[36] Stability is provided to the ULC via muco-periosteal, muco-perichondrial, and fibrous articulations to adjacent structures. At the dorsal aspect of the cephalic margin, the ULC joins the cartilaginous and bony septum and the nasal bones to form the keystone area. The cephalic portion of the ULC attaches to the undersurface of the nasal bones, overlapping by 6 to 8 mm.[37] The ULC is additionally attached to the pyriform aperture by the pyriform ligament, which contributes to the static support of the cartilaginous midvault.[38,39] Caudally, the ULC attaches to the LLC at the scroll area, which provides key structural support to the INV.[40,41]

Scroll Complex

The LLC cephalic edge turns down to form a hook, while the ULC caudal edge turns up to form a ledge. The 2 interdigitate, creating the characteristic scroll-like shape, and giving this region its name of "scroll" area or region.[42] There are numerous variations of this arrangement, and a keen understanding of the anatomic variations is essential for any intercartilaginous approaches to the nasal dorsum. Within this region complex, fibrous attachments are collectively referred to as the scroll ligament.[43] This complex includes a longitudinal scroll ligament which spans the junction between the ULC and LLC and is transected during intercartilaginous incisions. In addition, a vertical scroll ligament has been suggested, which connects the longitudinal scroll ligament to the overlying deep SMAS layer.[44]

The scroll complex is widely accepted as one of 3 major tip support mechanisms but also plays a significant role in nasal valve function. The scroll ligament provides support to the external valve by supporting and raising the caudal edge of the lateral crus of the LLC. Given its location at the lateral wall of the INV, the overlapping cartilages provide key structural stiffness. Additionally, the vertical scroll attachments to the overlying skin-soft tissue envelope provide further support to the INV.[45] Some authors advocate a subperichondrial dissection during rhinoplasty in order to elevate and preserve the overlying scroll ligaments.[46] Two prospective studies of open rhinoplasty patients found that scroll reconstruction was associated with improved nasal patency.[47,48]

Nasal Septum

The nasal septum is a vertical midline structure which separates the left and right nasal cavities, and is a composite structure of bone, cartilage, and mucosa. The quadrangular cartilage forms the anterior cartilaginous portion. Posteriorly, the perpendicular plate of ethmoid superiorly, the vomer inferiorly, and the nasal crest of the maxilla and palatine bones form the osseous portion. The vomer divides the choanae posteriorly, which separates the nasal cavity from the nasopharynx. The membranous septum, located anteriorly between the nasal columella and the caudal quadrangular cartilage, is formed by the union of septum mucous membranes and acts as a flexible buffer which may protect the cartilaginous septum[49]

Several classification systemsof septal deformities have been proposed. Multiple authors described deviations based on common patterns including a straight septal tilt, a C-shaped deformity, or an S-shaped deformity. For example, Guyuron described 6 classes of septal deviations, which includes the C- and S-shaped deformities each in the vertical and horizontal planes, the straight septal tilt, and a localized spur. Notable alternative classification systems include Rao and Mladina's description of 7 patterns of deviations, Baumann and Baumann's 6 types, and Buyukertan's division of the septum into 10 areas of interest.[50–54] Septal deviations may cause obstruction at various levels, and small deviations specifically in the region of the nasal valve cause significant narrowing of the INV angle.[55,56] Caudal deviations may also cause obstruction at the level of the ENV.

Inferior Turbinates

The 3 pairs of nasal turbinates arise from the lateral nasal sidewall, consisting of thin scrolls of bone covered in erectile tissue and mucoperiosteum. Whereas the superior and middle turbinates arise from the ethmoid bone, the inferior turbinates are separate bony structures. Covered in pseudostratified ciliated columnar epithelium, the bulk of the inferior turbinate is made of the lamina propria, which houses a rich network of venous sinusoids. This erectile tissue regulates the volume of the inferior turbinates in response to autonomic stimulation.[57] Inferior turbinate hypertrophy may be caused by enlargement of the bone, the mucosa, or both. Soft tissue hypertrophy is common and is typically seen in chronic rhinitis.[58]

PHYSIOLOGY

Airway Resistance

Airway resistance, the opposition to airflow, is defined by Ohm's law as the pressure gradient divided by the flow rate.

$$R = \frac{\Delta P}{Q}$$

With inspiration, a negative pressure gradient is generated between the nasopharynx and the nares, which causes air to flow through the nose with an inverse relationship to resistance. Thus, as resistance increases, flow decreases.

Nasal resistance may be measured by rhinomanometry, which uses a flow measuring device and 2 pressure sensors to measure pressure gradient. Active rhinomanometry uses physiologic airflow from the patient's own respiratory cycle, whereas passive rhinomanometry introduces extrinsic air typically via an air pump. Posterior rhinomanometry places a pressure sensor in the oral oropharynx, whereas anterior manometry places the sensor in the contralateral nasal cavity. Active anterior techniques are most common; active is more physiologic and anterior avoids the difficulty of the gag reflex.[59,60]

The significance of anatomic variations in determining the resistance of the nasal airway can be illustrated using Poiseuille's law, which describes the drop in pressure of laminar flow of an incompressible fluid in a long cylindrical pipe.

$$R = \frac{8\eta L}{\pi r^4}$$

Importantly, resistance varies inversely with the fourth power of the radius. A slight narrowing of the airway may cause an exponential increase in resistance. Given that the INV is the narrowest point of the nasal airway, any further reduction in CSA can greatly increase resistance, and significant attention has been focused on improving the patency of the INV.

Nasal Cycle

The nasal cycle refers to the spontaneous congestion and decongestion of the nasal mucosa, where the decongestion of one side is accompanied by the congestion of the contralateral side. Congestion of one side causes narrowing of the nasal airway, including at the INV and may contribute to nasal obstruction. First described by Kayser in 1895, the nasal cycle is driven by asymmetric blood flow to the erectile tissue in the nasal septum and inferior turbinate. The mechanisms which regulate blood flow are not clear, but significant attention has been focused on the autonomic nervous system. Sympathetic branches of the superior cervical ganglion give rise to the deep petrosal nerve, which joins parasympathetic preganglionic fibers from the greater superficial petrosal nerve to form the Vidian nerve. At the pterygopalatine ganglion, the parasympathetic fibers synapse with postganglionic neurons. Both sympathetic and parasympathetic fibers then travel along with nasal branches of the maxillary nerve (V2) through the sphenopalatine foramen to innervate the nasal mucosa.

These Vidian nerve fibers are targeted in patients with refractory rhinitis who continue to have rhinorrhea despite medical therapy. Historically, this involved resection of the neurovascular bundle at the level of the sphenopalatine foramen. While effective, Vidian neurectomy was also associated with cheek and palate numbness, dry eyes, and potentially unfavorable changes to the blood supply to the posterior nasal cavity. Instead, selective techniques which target postganglionic nerve branches have been proposed to reduce morbidity.[61,62] Various methods have been described, including surgical ablation, cryotherapy, and laser ablation. Radiofrequency ablation has received increasing interest, particularly since the Food and Drug Administration approval of the RhinAer radiofrequency system in 2020.[63,64]

Dynamic Collapse

Dynamic obstruction is lateral nasal sidewall collapse during inspiration. The Bernoulli principle explains that total airflow at any point along the nasal airway must be equal, and thus in narrower regions, velocity increases. Due to the conservation of energy, as velocity increases, a negative internal pressure is generated. Given that the INV is considered the narrowest point in the nasal airway, airflow reaches a maximum velocity at this point, leading to negative pressure which can lead to a transmural difference that overcomes the rigidity of the nasal sidewall and causes collapse. This collapse causes additional narrowing of the airway, which further increases resistance and decreases airflow.

Acoustic Rhinometry

Acoustic rhinometry is a noninvasive technique used to evaluate the geometry of the nasal cavity. A probe is sealed against a patient's nostril, a sound impulse is generated, and reflected sound waves are recorded. Changes in the CSA of the airway are assumed to correlate with changes in acoustic impedance. The time delay until the reflected sound is detected is used to calculate the distance traveled by the sound impulse along the airway. These data are used to generate CSA as a function of distance, and nasal cavity volume can be calculated as the integral of this curve.[65,66] Using acoustic rhinometry, previous studies have identified minimal cross-sectional areas (mCSAs) corresponding to 3 anatomic sources of obstruction, specifically the INV, the anterior half of the inferior and/or head of the middle turbinate, and the middle-posterior portion of the middle turbinate.[67,68] Unfortunately, acoustic rhinometry is not used routinely, due to significant experimental error, overestimation of the posterior nose due to sound leakage into the sinuses, and weak correlations between mCSA and nasal resistance.[69]

RETHINKING THE NASAL VALVE

The previous section represents the currently accepted concepts related to nasal airflow. Unfortunately, these principles rely on numerous assumptions which are invalid when considering normal human physiologic conditions. The nasal airway involves complex and dynamic interactions between airflow and a heterogeneous, collapsible structure.

Geometry

The idea of a critical INV angle of 10° to 15° is widely accepted, but most rhinoplasty surgeons would not approach nasal airway obstruction with a singular focus.[70] For one, the INV is not always a simple angle defined by 2 straight lines, but instead may be classified into several shapes and is sometimes occupied by the septal body.[71] Further, estimating the INV angle can vary significantly depending on the plane of measurement. For example, standard coronal CT images may significantly underestimate or overestimate the nasal valve angle compared with reformatted images which reflect the true orientation of the INV.[72] Even with the improved accuracy of reformatted images, measurements of the INV demonstrated no correlation to preoperative-modified Cottle maneuver scores, suggesting the limited clinical utility of the INV angle.[73]

Even when considering the 2D CSA of the INV rather than a simple angle, there is a poor correlation between mCSA and subjective scores of nasal patency.[74] The rate of persistent subjective symptoms after rhinoplasty remains high despite adequate increases in mCSA, affecting up to 53% of patients postoperatively.[75] Recent computational studies have suggested that the correlation between mCSA and resistance only becomes relevant below a critical area threshold which is only present in severely constricted nasal cavities. Therefore, in most patients, nasal resistance is significantly dependent on the geometry of regions throughout the nasal cavity other than the INV alone.[69,75]

The geometry of the nose is complex. Both Poiseuille's law and the Bernoulli principle describe flow through cylindrical pipes, but the shape of the nasal airway hardly resembles a cylinder and varies profoundly from one individual to another. Studies of nasal airflow unsurprisingly demonstrate significant inter-individual differences.[76] Computational fluid dynamics (CFD) has emerged as a technique to account for each patient's individual anatomy. A patient's CT scan is used to generate a 3D model of their individual nasal airway, which is then used to simulate nasal airflow. An example using an average nasal airflow created using statistical-shape modeling is shown in **Fig. 4**A–D, demonstrating the ability to calculate various parameters including airflow velocity, static pressure, and wall shear stress.[77] While their clinical applicability remains limited, these computational models have yielded significant new insights into nasal airflow physiology. For example, previous CFD studies have demonstrated that heat flux is a better correlate to subjective scores of obstruction.[78,79] Others have highlighted that the major flow path is through the middle meatus in some and through the inferior meatus in others, which may contribute to differences in perception of nasal airway patency.[80]

Reynolds Number

The Reynolds number is a nondimensional ratio of inertial forces to viscous forces within a fluid. At low Reynolds numbers, viscous forces dominate, leading to laminar flow in which fluid moves smoothly in layers without mixing perpendicular to the direction of flow. In contrast, at high Reynolds numbers, inertial forces dominate and produce a chaotic flow characterized by irregularity, eddies, and vortices. When describing flow through a long pipe, laminar flow typically occurs at Reynolds numbers less than 2300, turbulent flow at Reynolds numbers greater than 4000. Transitional flow, which is defined by central turbulent flow and peripheral laminar flow, occurs at intermediate Reynolds numbers between 2300 and 4000.

Nasal airflow is often accepted as laminar during "quiet" inspiration, however, this remains highly controversial. Estimates of the Reynolds number of nasal airflow range from 600 to 2000, however, the threshold at which flow becomes turbulent is

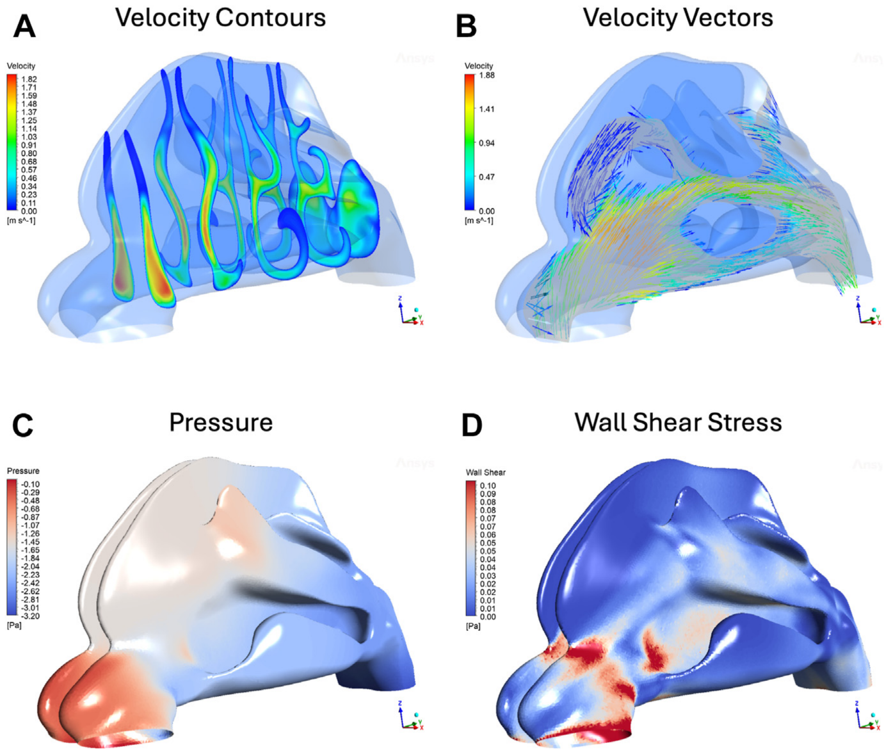

Fig. 4. CFD model of steady-state inspiration in an average nasal airway geometry. Multiple parameters can be calculated and visualized including (*A*) velocity contours at evenly spaced coronal planes, (*B*) velocity vectors along a para-sagittal plane demonstrating an anterior dorsal vortex, (*C*) static pressure distribution, and (*D*) wall shear stress.

dependent on the flow geometry.[80,81] Complex geometries may cause disruption in flow such that turbulence occurs at much lower Reynolds numbers within a range of 100 to 1000, with one study estimating a critical Reynolds of the nasal airway as low as 450.[82] Estimates of Reynolds number in the nasal airway often exceed this lower threshold, which implies transitional or turbulent flow even during quiet inspiration (**Fig. 5**). Turbulent flow is hypothesized to enhance heat and moisture transfer at the mucosa but also results in increased shear stress at the cavity walls and may lead to increased airway resistance.[70,83] Rather than describing the entire nasal cavity with a single Reynolds number, models which represent the valve and main nasal cavity as independent regions demonstrated higher accuracy, again highlighting the nuances of the complex nasal airway geometry.[84]

Fluid Structure Interaction

An accurate description of nasal airflow must account for the material properties of the nasal valve, which is a dynamic and collapsible structure.[85] The mechanical behavior of a material can be described by describing its change in response to an applied force, or load. These loads may be linear, including tensile or compressive loads which cause elongation or contraction respectively. The degree of deformation, referred to as strain, can be measured as a function of the force applied, referred to as stress. When a stress–strain curve is linear, the slope is known as the elastic modulus, or

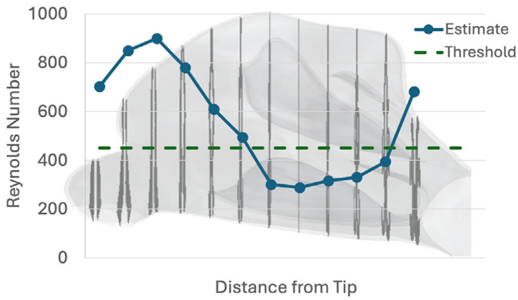

Fig. 5. Computational estimates of Reynolds number at evenly distributed cross-sections of the nasal airway. Anteriorly in the nasal valve region, these estimates exceed a lower threshold of 450 (*dashed line*).

Young's modulus, and describes the material's stiffness. When elongation or compression occurs, the material must also constrict or expand perpendicular to the direction of the applied stress. The tendency of a material to deform in direction perpendicular to a load is known as the Poisson's ratio.[86]

The currently accepted models of nasal valve physiology assume a static, rigid structure which does not account for the dynamic interactions between nasal airflow and the mobile nasal valve. Given the importance of dynamic valve collapse, there is a need for fluid-structure interaction (FSI) models, an extension of CFD, to incorporate the time-varying deformations of the nasal valve. By accounting for these material properties, one FSI model of the nasal valve during inspiratory sniffing conditions demonstrated good agreement with in vivo estimates of nasal valve collapse. Interestingly, they found that a dynamic model predicted a minimal increase in resistance of the nasal airway when compared with a model of the nasal airway as a static structure. In other words, during forceful inspiration, the increase in resistance caused by narrowing of the nasal valve and Poiseuille's law may be clinically insignificant.[87] Additional FSI models are warranted to investigate the contribution of dynamic valve collapse to nasal airway resistance, particularly during restful breathing.

Understanding the mechanisms of dynamic valve collapse is critical to surgical decision-making. Zoumalan and colleagues proposed a technique for real-time intraoperative assessment of the nasal valve, utilizing a suction at the nasal sill to generate a negative pressure. This produced airflow out of the nose in a direction analogous to expiration, while paradoxically causing depression of the nasal valve.[87] In a commentary, Rhee highlighted the obvious that physiologic expiration causes dilation of the nasal valve rather than collapse.[88] If the Bernoulli principle were accurately applied, then the INV should collapse as air flows into a narrowed segment, which should occur regardless of the direction of airflow during inspiration versus expiration. Alternatively, a simpler explanation may be that pressure inside the nasal airway is negative during inspiration and positive during expiration. With increasingly forceful nasal inspiration, negative pressure increases and overcomes the structural rigidity of the nasal sidewall, which is more similar to the Starling resistor commonly used to describe pharyngeal collapse in obstructive sleep apnea. The Bernoulli principle may still be relevant, but its relative significance is unclear. As Rhee noted, approaching surgery to increase the diameter of a "narrowed straw" is fundamentally different from approaching surgery to increase the rigidity of the lateral nasal wall.[88] Understanding the relevant importance of structural elasticity versus the Bernoulli principle is key to choosing the best surgical approach.

SUMMARY

The nasal valves are not simple, 2D cross-sections, but rather a complex, 3D, collapsible, and heterogenous structure. Nasal valve physiology has been often described with an emphasis on a critical INV angle, with the Bernoulli principle and Poiseuille's equation used to explain its singular significance in nasal obstruction. The geometry of the nasal airway is 3D and complex, however, and cannot be fully explained by our current understanding. As computational methods reveal new insights into nasal valve function, a new conceptual framework is needed to guide rhinoplasty surgical decision-making.

CLINICS CARE POINTS

- In addition to the cartilages and nasal bones, the skin and soft tissue envelope of the nose also plays a critical role in both form and function.
- Nasal valve dysfunction may be caused by septal deviations, turbinate hypertophy, and the shape and stiffness of the upper lateral cartilages. Identifying the correct sources of obstruction is key to a succesful surgical plan.
- Nasal obstruction is often more than simply a narrowed two-dimensional angle of the internal nasal valve. The nasal airway should be evaluated comprehensively with an appreciation for each patient's unique anatomy and geometry.

DISCLOSURE

The authors have nothing to close.

REFERENCES

1. Wexler DB, Davidson TM. The nasal valve: a review of the anatomy, imaging, and physiology. Am J Rhinol 2004;18:143–50.
2. Mink PJ. Physiologie Der Oberen Luftwege. Leipzig, Germany: F.C.W. Vogel; 1920.
3. Barrett DM, Casanueva FJ, Cook TA. Management of the nasal valve. Facial Plast Surg Clin North Am 2016;24(3):219–34.
4. Sinkler MA, Wehrle CJ, Elphingstone JW, et al. Surgical management of the internal nasal valve: a review of surgical approaches. Aesthetic Plast Surg 2021;45(3): 1127–36.
5. Hamilton GS. The external nasal valve. Facial Plast Surg Clin North Am 2017; 25(2):179–94.
6. Howard BK, Rohrich RJ. Understanding the nasal airway: principles and practice. Plast Reconstr Surg 2002;109(3):1128–46 [quiz: 1145–6].
7. GRIESMAN B. Muscles and cartilages of the nose from the standpoint of a typical rhinoplasty. Arch Otolaryngol Head Neck Surg 1944;39(4):334–41.
8. Hoeyberghs JL, Desta K, Matthews RN. The lost muscles of the nose. Aesthetic Plast Surg 1996;20(2):165–9.
9. Aksoy F, Veyseller B, Yildirim YS, et al. Role of nasal muscles in nasal valve collapse. Otolaryngol Head Neck Surg 2010;142(3):365–9.
10. Bruintjes TD, van Olphen AF, Hillen B, et al. Electromyography of the human nasal muscles. Eur Arch Oto-Rhino-Laryngol 1996;253(8):464–9.

11. Letourneau A, Daniel RK. The superficial musculoaponeurotic system of the nose. Plast Reconstr Surg 1988;82(1):48–57.
12. Bruintjes TD, Van Olphen AF, Hillen B, et al. A functional anatomic study of the relationship of the nasal cartilages and muscles to the nasal valve area. Laryngoscope 1998;108(7):1025–32.
13. Pou JD, Patel KG, Oyer SL. Treating nasal valve collapse in facial paralysis: what I do differently. Facial Plast Surg Clin North Am 2021;29(3):439–45.
14. Rohrich RJ, Malafa MM, Ahmad J, et al. Managing alar flare in rhinoplasty. Plast Reconstr Surg 2017;140(5):910–9.
15. Goffinet L, Barbier D, Lascombes P, et al. Nostrilplasty by manipulating the dilator naris muscles: a pilot study. Plast Reconstr Surg 2017;139(5):1208e–10e.
16. Hur MS, Hu KS, Youn KH, et al. New anatomical profile of the nasal musculature: dilator naris vestibularis, dilator naris anterior, and alar part of the nasalis. Clin Anat 2011;24(2):162–7.
17. Bruintjes TD, van Olphen AF, Hillen B. Review of the functional anatomy of the cartilages and muscles of the nose. Rhinology 1996;34(2):66–74. Available at: http://www.ncbi.nlm.nih.gov/pubmed/8876065.
18. Sakarya EU, Kar M, Bafaqeeh SA. Surgical anatomy of the external and internal nose. In: Cingi C, Muluk NB, editors. All around the nose. Cham, Germany: Springer International Publishing; 2020. p. 39–47. https://doi.org/10.1007/978-3-030-21217-9_4.
19. Soler ZM, Rosenthal E, Wax MK. Immediate nasal valve reconstruction after facial nerve resection. Arch Facial Plast Surg 2008;10(5):312–5.
20. Kienstra MA, Gassner HG, Sherris DA, et al. Effects of the nasal muscles on the nasal airway. Am J Rhinol 2005;19(4):375–81.
21. Lindsay RW, Bhama P, Hohman M, et al. Prospective evaluation of quality-of-life improvement after correction of the alar base in the flaccidly paralyzed face. JAMA Facial Plast Surg 2015;17(2):108–12.
22. Sheen JH, Sheen AP. Aesthetic rhinoplasty. St Louis, MO: CV Mosby; 1987.
23. Xavier R, Azeredo-Lopes S, Menger DJ, et al. Cephalic malposition of the lateral crura and parenthesis deformity: a cadaver study in caucasians. Aesthetic Plast Surg 2020;44(6):2244–52.
24. Toriumi DM, Asher SA. Lateral crural repositioning for treatment of cephalic malposition. Facial Plast Surg Clin North Am. 2015;23(1):55–71.
25. Constantian MB, Clardy RB. The relative importance of septal and nasal valvular surgery in correcting airway obstruction in primary and secondary rhinoplasty. Plast Reconstr Surg 1996;98(1):38–54 [discussion: 55–8].
26. Constantian MB. The two essential elements for planning tip surgery in primary and secondary rhinoplasty: observations based on review of 100 consecutive patients. Plast Reconstr Surg 2004;114(6):1571–81 [discussion: 1582–5].
27. Constantian MB. Functional effects of alar cartilage malposition. Ann Plast Surg 1993;30(6):487–99.
28. Gunter JP, Friedman RM. Lateral crural strut graft: technique and clinical applications in rhinoplasty. Plast Reconstr Surg 1997;99(4):943–52 [discussion: 953–5].
29. Bared A, Rashan A, Caughlin BP, et al. Lower lateral cartilage repositioning objective analysis using 3-dimensional imaging. JAMA Facial Plast Surg 2014;16(4):261–7.
30. Davis RE. Lateral crural tensioning for refinement of the wide and underprojected nasal tip: rethinking the lateral crural steal. Facial Plast Surg Clin North Am 2015;23(1):23–53.

31. Best CAE, Wong BJF. Nasal valve management: the case to move away from grafts to tensioning. Curr Otorhinolaryngol Rep 2023;11(3):260–5.
32. Kondo M, Orgain C, Alvarado R, et al. The effects of lateral crural tensioning with an articulated alar rim graft versus lateral crural strut graft on nasal function. Facial Plast Surg Aesthet Med 2020;22(4):281–5.
33. Goodrich JL, Wong BJF. Optimizing the soft tissue triangle, alar margin furrow, and alar ridge aesthetics: analysis and use of the articulate alar rim graft. Facial Plast Surg 2016;32(6):646–55.
34. Foulad A, Volgger V, Wong B. Lateral crural tensioning for refinement of the nasal tip and increasing alar stability: a case series. Facial Plast Surg 2017;33(3): 316–23.
35. Hismi A, Burks CA, Locascio JJ, et al. Comparative effectiveness of cartilage grafts in functional rhinoplasty for nasal sidewall collapse. Facial Plast Surg Aesthet Med 2022;24(3):240–6.
36. Toriumi DM. Management of the middle nasal vault in rhinoplasty. Operative Techniques in Plast Reconstr Surg 1995;2(1):16–30.
37. Rohrich RJ, Adams WP, Ahmad J, et al. Dallas rhinoplasty nasal surgery by the masters. New York, NY: Thieme Medical Pub; 2014.
38. Rohrich RJ, Hoxworth RE, Thornton JF, et al. The pyriform ligament. Plast Reconstr Surg 2008;121(1):277–81.
39. Craig JR, Bied A, Landas S, et al. Anatomy of the upper lateral cartilage along the lateral pyriform aperture. Plast Reconstr Surg 2015;135:406–11.
40. Janeke JB, Wright WK. Studies on the support of the nasal tip. Arch Otolaryngol 1971;93(5):458–64.
41. Saban YC, Amodeo A, Hammou JC, et al, An anatomical study of the nasal superficial musculoaponeurotic system surgical applications in rhinoplasty. Vol 10, Available at: www.liebertpub.com, (Accessed 18 May 2024), 2008.
42. Cunningham B, McKinney P. The alar scroll: an important anatomical structure in lobule surgery. Operat Tech Plast Reconstr Surg 2000;7(4):187–93.
43. Daniel RK, Palhazi P. The nasal ligaments and tip support in rhinoplasty: an anatomical study. Aesthet Surg J 2018;38(4):357–68.
44. Saban Y, Andretto Amodeo C, Hammou JC, et al. An anatomical study of the nasal superficial musculoaponeurotic system: surgical applications in rhinoplasty. Arch Facial Plast Surg 2008;10(2):109–15.
45. Bitik O, Uzun H, Konaş E. Scroll reconstruction: fine tuning of the interface between middle and lower thirds in rhinoplasty. Aesthet Surg J 2019;39(5):481–94.
46. Çakir B, Öreroğlu AR, Doğan T, et al. A complete subperichondrial dissection technique for rhinoplasty with management of the nasal ligaments. Aesthet Surg J 2012; 32(5):564–74.
47. Barone M, Salzillo R, De Bernardis R, et al. Reconstruction of scroll and pitanguy's ligaments in open rhinoplasty: a controlled randomized study. Aesthetic Plast Surg 2023. https://doi.org/10.1007/s00266-023-03725-0.
48. Ozturk A, Eroglu S, Timur B, et al. Functional role of scroll reconstruction in open rhinoplasty. Aesthetic Plast Surg 2021. https://doi.org/10.1007/s00266.
49. Stovin JS. The importance of the membranous nasal septum. AMA Arch Otolaryngol 1958;67(5):540.
50. Mladina R, Čujić E, Šubarić M, et al. Nasal septal deformities in ear, nose, and throat patients. An international study. American Journal of Otolaryngology - Head and Neck Medicine and Surgery 2008;29(2):75–82.

51. Lin JK, Wheatley FC, Handwerker J, et al. Analyzing nasal septal deviations to develop a new classification system: a computed tomography study using MATLAB and OsiriX. JAMA Facial Plast Surg 2014;16(3):183–7.
52. Buyukertan M, Keklikoglu N, Kokten G. A morphometric consideration of nasal septal deviations by people with paranasal complaints; a computed tomography study. Rhinology 2003;41(1):21–4. Available at: http://www.ncbi.nlm.nih.gov/pubmed/12677736.
53. Baumann I, Baumann H. A new classification of septal deviations. Rhinology 2007;45(3):220–3. Available at: http://www.ncbi.nlm.nih.gov/pubmed/17956023.
54. Guyuron B, Uzzo CD, Scull H. A practical classification of septonasal deviation and an effective guide to septal surgery. Plast Reconstr Surg 1999;104(7): 2202–9 [discussion: 2210–2].
55. Fettman N, Sanford T, Sindwani R. Surgical management of the deviated septum: techniques in septoplasty. Otolaryngol Clin North Am 2009;42(2):241–52.
56. Clark DW, Signore AG Del, Raithatha R, et al, Nasal airway obstruction: prevalence and anatomic contributors. Vol 97, Available at: www.entjournal.com173, (Accessed 28 April 2024).
57. Berger G, Balum-Azim M, Ophir D. The normal inferior turbinate: histomorphometric analysis and clinical implications. Laryngoscope 2003;113(7):1192–8.
58. Hsu DW, Suh JD. Anatomy and physiology of nasal obstruction. Otolaryngol Clin North Am 2018;51(5):853–65.
59. Naito K, Horibe S, Tanabe Y, et al. Objective assessment of nasal obstruction. Fujita medical journal 2023;9(2):53–64.
60. Clement PAR, Gordts F. Standardisation committee on objective assessment of the nasal airway I and E. Consensus report on acoustic rhinometry and rhinomanometry. Rhinology 2005;43(3):169–79.
61. Kikawada T. Endoscopic posterior nasal neurectomy: an alternative to vidian neurectomy. Operat Tech Otolaryngol Head Neck Surg 2007;18(4):297–301.
62. Takahara D, Takeno S, Hamamoto T, et al. Management of intractable nasal hyperreactivity by selective resection of posterior nasal nerve branches. Int J Otolaryngol 2017;2017:1–5.
63. Yu AJ, Tam B, Wrobel B, et al. Radiofrequency neurolysis of the posterior nasal nerve: a systematic review and meta-analysis. Laryngoscope 2024;134(2): 507–16.
64. Stolovitzky JP, Ow RA, Silvers SL, et al. Effect of radiofrequency neurolysis on the symptoms of chronic rhinitis: a randomized controlled trial. OTO Open 2021;5(3). https://doi.org/10.1177/2473974X211041124.
65. Roithmann R, Cole P, Chapnik J, et al. Acoustic rhinometry in the evaluation of nasal obstruction. Laryngoscope 1995;105(3):275–81.
66. Hilberg O, Jackson AC, Swift DL, et al. Acoustic rhinometry: evaluation of nasal cavity geometry by acoustic reflection. J Appl Physiol (1985) 1989;66(1): 295–303.
67. Mamikoglu B, Houser SM, Corey JP. An interpretation method for objective assessment of nasal congestion with acoustic rhinometry. Laryngoscope 2002; 112(5):926–9.
68. Corey JP. Acoustic rhinometry: should we be using it? Curr Opin Otolaryngol Head Neck Surg 2006;14(1):29–34.
69. Garcia GJM, Hariri BM, Patel RG, et al. The relationship between nasal resistance to airflow and the airspace minimal cross-sectional area. J Biomech 2016;49(9): 1670–8.

70. Tripathi PB, Elghobashi S, Wong BJF. The myth of the internal nasal valve. JAMA Facial Plast Surg 2017;19(4):253–4.
71. Miman MC, Deliktaş H, Özturan O, et al. Internal nasal valve: revisited with objective facts. Otolaryngol Head Neck Surg 2006;134(1):41–7.
72. Poetker DM, Rhee JS, Mocan BO, et al. Computed tomography technique for evaluation of the nasal valve. Arch Facial Plast Surg 2004;6(4):240–3.
73. Bloom JD, Sridharan S, Hagiwara M, et al. Reformatted computed tomography to assess the internal nasal valve and association with physical examination. Arch Facial Plast Surg 2012;14:331–5. Available at: www.liebertpub.com.
74. André RF, Vuyk HD, Ahmed A, et al. Correlation between subjective and objective evaluation of the nasal airway. A systematic review of the highest level of evidence. Clin Otolaryngol 2009;34(6):518–25.
75. Campbell DA, Moghaddam MG, Rhee JS, et al. Narrowed posterior nasal airway limits efficacy of anterior septoplasty. Facial Plast Surg Aesthet Med 2021;23(1):13–20.
76. Segal RA, Kepler GM, Kimbell JS. Effects of differences in nasal anatomy on airflow distribution: a comparison of four individuals at rest. Ann Biomed Eng 2008;36(11):1870–82.
77. Brüning J, Hildebrandt T, Heppt W, et al. Characterization of the airflow within an average geometry of the healthy human nasal cavity. Sci Rep 2020;10(1). https://doi.org/10.1038/s41598-020-60755-3.
78. Kimbell JS, Frank DO, Laud P, et al. Changes in nasal airflow and heat transfer correlate with symptom improvement after surgery for nasal obstruction. J Biomech 2013;46(15):2634–43.
79. Sullivan CD, Garcia GJM, Frank-Ito DO, et al. Perception of better nasal patency correlates with increased mucosal cooling after surgery for nasal obstruction. Otolaryngol Head Neck Surg 2014;150(1):139–47.
80. Zhao K, Jiang J. What is normal nasal airflow? A computational study of 22 healthy adults. Int Forum Allergy Rhinol 2014;4(6):435–46.
81. Johnsen SG. Computational rhinology: unraveling discrepancies between in silico and in vivo nasal airflow assessments for enhanced clinical decision support. Bioengineering 2024;11(3). https://doi.org/10.3390/bioengineering11030239.
82. O'neill G, Tolley NS. Modelling nasal airflow coefficients: an insight into the nature of airflow. Rhinology 2021;59(1):66–74.
83. Chen XB, Lee HP, Chong VFH, et al. Assessment of septal deviation effects on nasal air flow: a computational fluid dynamics model. Laryngoscope 2009;119(9):1730–6.
84. O'neill G, Tolley NS. The complexities of nasal airflow: theory and practice. J Appl Physiol 2019;127:1215–23.
85. Shi B, Huang H. Computational technology for nasal cartilage-related clinical research and application. Int J Oral Sci 2020;12(1). https://doi.org/10.1038/s41368-020-00089-y.
86. Callister Jr WD, Rethwisch DG. Materials science and engineering: an introduction. 10th edition. Wiley; 2018.
87. Zoumalan RA, Larrabee WF, Murakami CS. Intraoperative suction-assisted evaluation of the nasal valve in rhinoplasty. Arch Facial Plast Surg 2012;14(1):34–8.
88. Rhee JS, Kimbell JS. The nasal valve dilemma: the narrow straw vs the weak wall. Arch Facial Plast Surg 2012;14(1):9–10.